Are there different types of error monitoring? A microstates analysis of error-related brain activity across three tasks

Anna Grabowska (anna.belowska@doctoral.uj.edu.pl)
Doctoral School in the Social Sciences, Rynek Głowny 34, 31-010 Krakow, Poland
Centre for Cognitive Science, Ingardena 3, 30-060 Krakow, Poland

Filip Sondej (filip.sondej@uj.edu.pl)
Centre for Cognitive Science, Ingardena 3, 30-060 Krakow, Poland

Magdalena Senderecka (magdalena.senderecka@uj.edu.pl)
Centre for Cognitive Science, Ingardena 3, 30-060 Krakow, Poland

Abstract

Error monitoring is commonly studied using various inhibitory control tasks, involving response withholding, response cancellation, or response selection. However, it remains unclear whether there is a common neural mechanism underlying error monitoring across these tasks or if it is specific to distinct types of cognitive failures. To identify both similarities and differences in the neural processing of errors across go/no-go, stop-signal, and flanker tasks, we employed microstate analysis. This method allows to study the dynamically evolving topographical patterns of neural activity throughout the brain. Our results revealed that the early phase of error monitoring in all tasks predominantly engages the supplementary motor area. In addition, we observed task-specific neural activity encompassing visual and motor areas in the go/no-go task, the dorsal part of the anterior cingulate cortex in the stop-signal task, and its ventral part in the flanker task. These findings suggest that error monitoring involves a collection of interconnected cognitive processes, rather than a uniform mechanism across tasks.

Keywords: error monitoring, response inhibition, error-related negativity, electroencephalography, microstates

Introduction

The continuous monitoring of action outcomes, particularly erroneous ones, is essential for adaptive adjustments (Ullsperger, Danielmeier, & Jocham, 2014). Excessive error monitoring has been observed in conditions like generalized anxiety disorder and obsessive-compulsive disorder (Endrass & Ullsperger, 2014; Olvet & Hajcak, 2008; Riesel, 2019), while diminished error monitoring has been widely reported in a range of externalizing disorders, such as attention-deficit hyperactivity disorder (Senderecka et al., 2012; van Meel et al., 2007) or schizophrenia (Foti et al., 2012).

Error monitoring is typically measured in paradigms involving inhibitory control, such as the Stroop (1935), flanker (Eriksen & Eriksen, 1974), stop-signal (Logan & Cowan, 1984), and go/no-go (Rosvold et al., 1956) tasks. These tasks require a response to a target stimulus among irrelevant or distracting stimuli. However, errors in different inhibitory control tasks arise from failures in distinct cognitive processes. For example, errors in the go/no-go task typically result from failures to withhold a response, while in the stop-signal task, errors occur due to the failure to cancel an already initiated response. In the Flanker or Stroop tasks errors often stem from difficulties in selecting the correct response when faced with conflicting stimuli. Although response withholding, cancellation, and selection rely on overlapping cognitive and neural mechanisms, they are distinct processes that also engage task-specific neural systems (Swick, Ashley, & Turken, 2011; Zhang, Geng, & Lee, 2017).

The variability in neural activity across inhibitory control types raises a key question: Are failures in response withholding, cancellation, and selection processed similarly, and error monitoring reflects a general neural mechanism, or is it domain-specific process linked to types of cognitive failures?

The assumption of functional equivalence of error monitoring across tasks was previously studied, among others, by Segalowitz et al. (2010) and Riesel et al. (2013) and more recently investigated by Clayson et al. (2023). These studies primarily focused on error-related negativity (ERN; Gehring et al., 1993), a well-established neural correlate of error monitoring. The ERN is an event-related potential (ERP) component derived from electroencephalographic (EEG) signals, which manifests as a negative deflection peaking 50–100 ms after an error occurs. Evidence from both functional magnetic resonance imaging and EEG research identifies the anterior cingulate cortex (ACC), particularly its dorsal region (dACC; Brazdil et al., 2005; Dehaene, Posner, & Tucker, 1994), as the primary neural source of the ERN. More recently, motor-related regions, including the supplementary motor area (SMA; Bonini et al., 2014) and pre-SMA (Fu et al., 2019; Iannaccone et al., 2015), have also been implicated as ERN generators.

Riesel et al. (2013) analyzed correlations between ERNs recorded during go/no-go, flanker, and Stroop tasks, finding that the bivariate Pearson correlations between ERNs across these tasks were approximately 0.38. Clayson and colleagues (2023) conducted a registered replication of Riesel et al.'s study (N = 182), finding bivariate correlations around 0.50. The strongest correlation was observed between the flanker and go/no-go tasks (r = 0.57). These findings suggest that approximately 40–50% of the ERN's variance is shared across tasks requiring response withholding and selection, while the remaining variance reflects task-specific processes.

Riesel et al. suggested that the observed within-individual correlations between ERNs across tasks may be driven by anatomical convergence in the neural networks underlying error monitoring across different contexts. However, they did

In D. Barner, N.R. Bramley, A. Ruggeri and C.M. Walker (Eds.), *Proceedings of the 47th Annual Conference of the Cognitive Science Society*

not specify which brain regions are responsible for the shared or context-related variance. In the present study, we aim to address this gap and explore how the neuroanatomical correlates of the ERN overlap or can be dissociated across tasks.

Previous research has predominantly focused on ERN mean or peak amplitude as a biomarker of error monitoring. However, relying on single-electrode EEG signals does not allow for the identification of neural sources underlying amplitude differences across tasks. Rather than solely reflecting the intensity of error-monitoring, these differences may stem from variability in both spatial and temporal dynamics. Additionally, they may also arise when distinct, task-specific neural processes are misidentified as the same.

To directly address this issue, we applied a microstate approach to analyze the EEG signal recorded during error commission in the go/no-go, stop-signal, and flanker tasks. This method enabled us to explore both common and distinct spatiotemporal neural patterns underlying error processing across response withholding (go/no-go), cancellation (stop-signal), and selection (flanker).

The microstate approach has gained increasing popularity in recent years as a tool for studying the temporal dynamics of both resting-state (Bréchet et al., 2020; Nash et al., 2022) and event-related neural processes (Antonova et al., 2021). Microstates are patterns of scalp potential topographies identified through clustering algorithms, which remain stable in spatial location and typically last 20–150 ms (Michel & Koenig, 2018). Since these patterns are believed to reflect specific mental processes, microstate analysis enables the identification and source localization of functional neural networks linked to distinct cognitive processes. Recently, it has been successfully applied in error monitoring research to uncover neural sources of error-related brain activity following anxiety interventions (Nash et al., 2023), and to identify common patterns between resting-state and error-related neural activity (Bagdasarov et al., 2024).

The goal of the current study is to identify the cognitive processes involved in error processing across go/no-go, stop-signal, and flanker tasks. By adopting this approach, we aim to precisely determine how, where, and when both general and task-specific error monitoring processes occur across different types of inhibitory control.

Materials and Methods

Participants

A total of 225 volunteers (113 F) aged 18–39 (M = 23.64, SD = 4.18) with normal or corrected-to-normal vision were recruited from the general population via internet advertisements. Seventeen participants were excluded for the following reasons: lack of EEG data due to technical issues (N = 1); fewer than five committed errors in any of the tasks (N = 4); or fewer than five trials with erroneous response after artifact rejection in any of the tasks (N = 12). The final sample consisted of 208 participants (105 F), aged 18–39 (M = 23.60, SD = 4.14).

Procedure and tasks

Participants received verbal and written information about the purpose and procedure of the study. While the EEG signal was recorded, they completed a speeded color and orientation go/no-go discrimination task, which has been validated in several previous studies (Grabowska, Sondej, & Senderecka, 2024; Pourtois, 2011; Vocat, Pourtois, & Vuilleumier, 2008), a stop-signal task with stop-signal delays continuously adjusted using a standard adaptive tracking procedure (Verbruggen et al., 2019), and a speeded, modified version of the flanker task, also validated in previous research (Fiehler et al., 2005; Grabowska et al., 2025; Ullsperger & von Cramon, 2001). Responses were made with both hands, except the go/no-go task, where only the right hand was used. The study was conducted in accordance with the Declaration of Helsinki (BMJ, 1996), and the protocol was approved by the local Research Ethics Committee. All participants provided written informed consent and were compensated monetarily for their time. The same sample was included in the research described in Grabowska, Zabielski, and Senderecka (2024); Grabowska et al. (2024); Grabowska et al. (2025).

Electrophysiological recording and data pre-processing

The EEG signal was continuously recorded at 256 Hz from 64 silver/silver-chloride (Ag/AgCl) active electrodes (with preamplifiers) using the BioSemi Active-Two system and referenced online to CMS-DRL ground. Off-line, the signal was re-referenced to the average of the left and right mastoid electrodes, band-pass filtered between 0.05 Hz and 25 Hz with a Butterworth filter, and notch filtered at 50 Hz, to remove the power-line noise. Data were further segmented into 700 ms epochs around the response onset (-100 to 600 ms) and baseline corrected to the average of -100 to 0 ms pre-response activity. Blinks were removed using the Gratton, Coles, and Donchin (1983) algorithm. Noise epochs were rejected via an automatic procedure, with rejection criteria of ±75 μV. Epochs were then re-baselined and divided into correct-response and error-response trials.

For each participant and task, artifact-free trials with erroneous response were averaged (M = 27.27, SD = 13.93 trials for the go/no-go task; M = 44.03, SD = 9.99 trials for the stop-signal task; M = 30.48, SD = 15.14 trials for the flanker task). On average, 4.58 (SD = 5.88), 6.57 (SD = 7.48), and 4.43 (SD = 6.20) error trials were excluded during preprocessing due to artifacts in the go/no-go, stop-signal, and flanker tasks, respectively. ERN amplitudes were quantified as the mean activity from 0 to 100 ms at Fz for the go/no-go task and FCz for the stop-signal and flanker tasks. We selected the electrodes where the ERN amplitude was maximal, following previous studies (Hajcak et al., 2008; Ridderinkhof et al., 2003).

Microstate analyses

The microstate analysis was performed using CARTOOL (Brunet, Murray, & Michel, 2011). Population-level grand-average error-locked ERPs were computed separately for

the go/no-go, stop-signal, and flanker tasks and subjected to a spatial k-means clustering analysis (random trials = 300). This method minimized global map dissimilarity between maps to identify the most dominant topographies in the grand-average ERPs across the three tasks. Segmentation was conducted using the following parameters: rejecting segments shorter than 5 time points (∼20 ms) and clustering within a range of 1 to 10 clusters per task. The optimal solution, comprising 14 clusters, was determined based on a meta-criterion analysis. The ERN-related microstate was identified through visual inspection of the cluster results.

All 14 group-level microstates were then backfitted to individual ERPs by assigning each ERP time point to the best-matching microstate, yielding individual-level segmentations. We then calculated mean global field power (mGFP) for each individual-level microstate as an indicator of its intensity.

Source localization

To analyze the cortical sources of error-related microstates in the go/no-go, stop-signal, and flanker tasks, we used standardized Low Resolution Brain Electromagnetic Tomography (sLORETA; Pascual-Marqui, 2002). The sLORETA solution space had a voxel size of 6 × 6 × 6 mm, defined by the digitized Montreal Neurological Institute (MNI) probability atlas. For each participant and task, sLORETA images were computed for individual-level ERN-related microstate at each time point. The results were regularized to account for background EEG noise and enforce smoothness and were normalized to correct for variability in EEG power over time (Michel & Brunet, 2019). Then, the dipole amplitudes were averaged across time points.

To enhance the interpretation and visualization of microstate sources and their overlap, source maps were converted into volumes and analyzed with AFNI (Cox, 1996). Activation cluster coordinates are reported in MNI space, along with corresponding Brodmann area (BA) locations. Sources within the cerebellum and subcortical structures were excluded from the analysis due to the limited validity of measuring the activity of these regions with EEG (Bagdasarov et al., 2022).

Statistical analyses

In an initial analysis, we examined whether ERN mean amplitudes were correlated across go/no-go, stop-signal, and flanker tasks using Pearson correlation.

We then used mixed-effects modeling to confirm that the identified error-related microstates were related to the typically measured ERN mean amplitude. ERN amplitude was modeled as a function of ERN-related microstate mGFP, task type, and their interaction, with a random intercept for each participant. The model specification was as follows:

$$\text{ERN} \sim \text{microstate GFP} * \text{Task} + (1|\text{Participant})$$

To initially assess the consistency of error monitoring in response withholding, cancellation, and selection, we conducted paired-samples t-tests to examine whether the mGFP of identified ERN-related microstates differed across tasks.

To further investigate the common and distinct neural mechanisms underlying error monitoring in response withholding, cancellation, and selection, we analyzed sLORETA images from the identified ERN-related microstates. Specifically, we aimed to (1) identify overlapping ERN-related activation patterns across different types of response inhibition tasks, and (2) estimate task contrasts (go/no-go vs flanker, go/no-go vs stop-signal, and flanker vs stop-signal) using sLORETA images to isolate brain regions specifically associated with the early phase of error monitoring in each type of inhibitory control. To compare task-related activity, whole-brain voxel-by-voxel paired t-tests were conducted on the individual-level ERN-related microstates with False Discovery Rate (FDR) correction.

Results

Behavioral results

The average number of erroneous responses per participant was: 31.85 (*SD* = 14.27) in the go/no-go task, 50.66 (*SD* = 7.50) in the stop-signal task, and 32.83 (*SD* = 14.40) in the flanker task. In the go/no-go task, the average response time (RT) per participant for erroneous responses was 263 ms (*SD* = 35 ms), while for correct responses it was 303 ms (*SD* = 33 ms). In the stop-signal task, the average RT for erroneous responses (uninhibited) was 349 ms (*SD* = 35 ms), and for correct responses, it was 399 ms (*SD* = 54 ms). In the flanker task, the average RT for erroneous responses (across both congruent and incongruent trials) was 233 ms (*SD* = 30 ms), and for correct responses, it was 288 ms (*SD* = 33 ms). As expected, participants responded significantly faster on error trials relative to correct trials in all three tasks (all $p < .001$). The average inhibition rate, defined as the ratio of correctly inhibited responses to total inhibition attempts, was 0.72 (*SD* = 0.13) for the go/no-go task, and 0.49 (*SD* = 0.07) for the stop-signal task. For the flanker task, the average successful conflict resolution, defined as the ratio of correct responses in incongruent trials to the total number of incongruent trials was 0.63 (*SD* = 0.16).

ERP measures

The average ERN amplitude was -3.58 μV (*SD* = 4.49 μV) in the go/no-go task, -2.53 μV (*SD* = 4.48 μV) in the stop-signal task, and -4.21 μV (*SD* = 5.38 μV) in the flanker task.

To assess the similarity of ERN amplitudes across tasks, we computed bivariate Pearson correlations. The correlation between ERN amplitudes in the go/no-go and flanker tasks was 0.53 (95% CI [0.43, 0.62]), in the go/no-go and stop-signal tasks was 0.45 (95% CI [0.33, 0.55]), and in the stop-signal and flanker tasks was 0.61 (95% CI [0.52, 0.69]).

Microstate analysis

The meta-criterion identified a 14-microstate solution as the optimal model for describing error-related brain activity

across the go/no-go, stop-signal, and flanker tasks (Fig. 1). The ERN-related microstates of interest were those within the typical ERN 0 - 100 ms time window, showing a fronto-central distribution. Based on their temporal and spatial distributions, we identified microstate 6 as the ERN-related microstate for the go/no-go and flanker tasks and microstate 7 as the ERN-related microstate for the stop-signal task. Microstate 6 lasts from 0 to 100 ms in the go/no-go task and from -9 to 91 ms in the flanker task, exhibiting strong fronto-central negativity corresponding to the classic ERN. Microstate 7 lasts from 9 to 103 ms in the stop-signal task, also displaying characteristic central negativity.

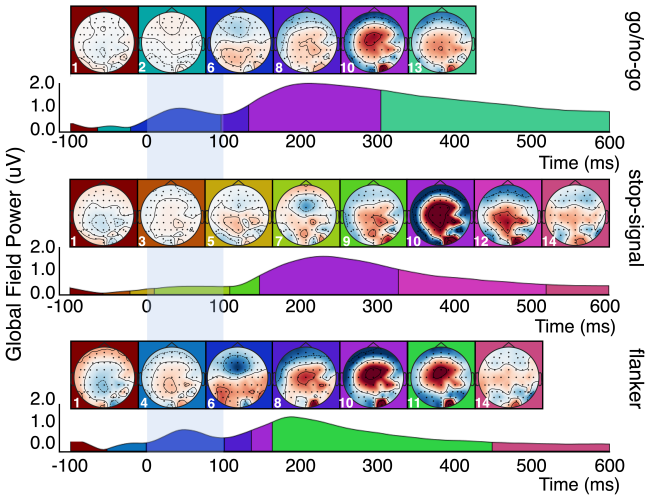

Figure 1: Microstate sequences in response to error commission in the go/no-go, stop-signal, and flanker tasks from -100 to 600 ms after error commission. The highlighted shaded blue area represents expected time period for ERN-related microstates.

The microstate templates revealed in the group-level analysis were then backfitted to the individual grand average error-locked ERPs. After the backfitting procedure, in the -50 to 100 ms time window, 189 participants had ERN-related microstate 6 in the go/no-go task, 147 in the stop-signal task, and 187 in the flanker task. In contrast, 16 participants had ERN-related microstate 7 in the go/no-go task, 77 in the stop-signal task, and 20 in the flanker task.

We then validated the similarity between the identified ERN-related microstates and the ERNs using a mixed-effects model. Additionally, we estimated the association between the mGFP of microstate 6 and ERN amplitude in the stop-signal task, as both microstates 6 and 7 equally accounted for the stop-signal data.

The mixed-effects model revealed a significant association between the mGFP of ERN-related microstates and ERN amplitude across tasks (b = -4.46, p <0.001, 95% CI [-6.04, -2.88]), with higher mGFP corresponding to lower (more negative) ERN amplitude. Go/no-go was set as the reference task, and no significant differences were found between the go/no-go and flanker tasks (p = 0.635). However, the interaction effect for the stop-signal task was significant (b = 2.30, p = 0.023, 95% CI [0.32, 4.28]), suggesting a weaker association between the stop-signal ERN-related microstate 7 and ERN amplitude compared to the go/no-go task. Similar results were obtained with mGFP of microstate 6.

We then examined the differences between ERN-related microstates across tasks. Paired t-tests revealed that participants in the flanker task showed increased mGFP for microstate 6 (M = 0.81 μV^2, SD = 0.36) compared to the go/no-go task (M = 0.71 μV^2, SD = 0.31), t(207) = -2.94, p = 0.004, and to the stop-signal microstate 7 (M = 0.28 μV^2, SD = 0.38), t(207) = 15.36, p <0.001. Additionally, participants in the go/no-go task showed increased mGFP for microstate 6 compared to the mGFP for microstate 7 in the stop-signal task, t(207) = 12.86, p <0.001. These results align with the relationships observed between ERN mean amplitudes across tasks, confirming the relation between ERN amplitudes and ERN-related microstates.

Source localization of microstates

The microstate analysis revealed that, although the early phase of error monitoring in the go/no-go and flanker tasks was associated with the same microstate, the intensity of the underlying neural activity differed between the tasks. In contrast, the early phase of error monitoring in the stop-signal task was linked to a different microstate than the one observed in the go/no-go and flanker tasks. To further investigate the neural origins of these differences, we conducted sLORETA analyses to source-localize microstate 6 in the go/no-go and flanker tasks and microstate 7 in the stop-signal task. Figure 2 shows the results of the sLORETA analysis.

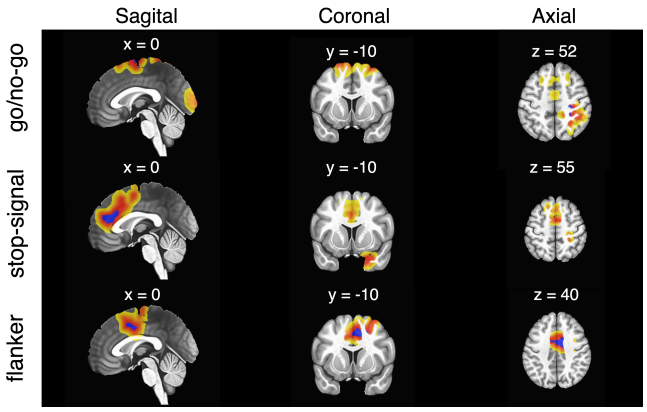

Figure 2: Neural sources of error-related microstate 6, extracted from the go/no-go and flanker tasks, and microstate 7, extracted from the stop-signal task using sLORETA. The blue color indicates the cluster with the highest activity.

In the go/no-go task, the largest cluster of 132,096 voxels included the primary motor cortex (BA 4), premotor cortex and SMA (BA 6), somatosensory association cortex (BA 5), and visuo-motor areas (BA 7), with the center of mass

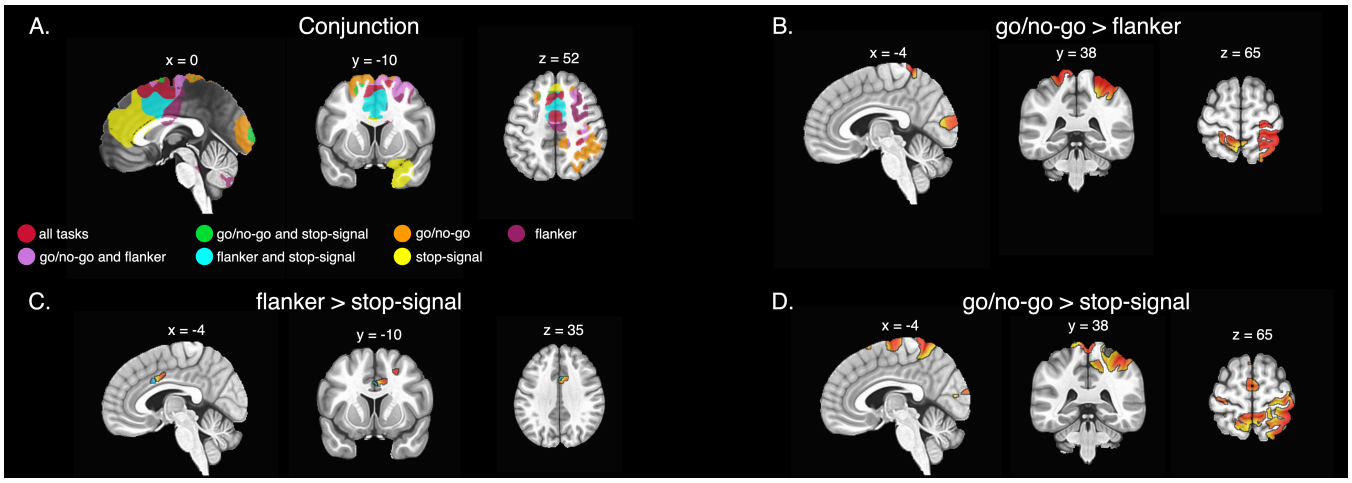

Figure 3: Comparison of neural sources across tasks. A) Common and distinct areas activated across tasks. B) Brain activations for the go/no-go task contrasted with the flanker task. C) Brain activations for the flanker task contrasted with the stop-signal task. D) Brain activations for the go/no-go task contrasted with the stop-signal task.

at MNI coordinates (XYZ) = -8.7, 25.2, 66.2 (left primary motor cortex). Additional clusters of activation were found in the left visual areas (BA 17–19). In the flanker task, the largest cluster of 71,124 voxels included the premotor cortex and SMA (BA 6) and ventral ACC (BA 24), with the center of mass at MNI coordinates (XYZ) = -7.5, -2.2, 49.4 (SMA). Additional clusters included the primary motor cortex (BA 4), somatosensory association cortex (BA 5), visuo-motor areas (BA 7), primary sensory areas (BA 1), superior temporal gyrus (BA 22), and auditory cortex (BA 41). In the stop-signal task, the main cluster of 94,112 voxels included the dACC (BA 32), with the center of mass at MNI coordinates (XYZ) = -1.3, -29.0, 31.4. Additional activation clusters included the parahippocampal gyrus (BA 36), temporal pole (BA 38), somatosensory association cortex (BA 5), visual areas (BA 18), primary sensory areas (BA 1), anterior prefrontal cortex (BA 10), and premotor cortex and SMA (BA 6).

Figure 3, panel A, shows the overlapping areas across tasks. The main cluster activated in all three tasks involved the left and right premotor cortex and SMA (BA 6; the center of mass at MNI coordinates (XYZ) = -4.6, -7.1, 59.3), left primary sensory areas (BA 1), primary motor cortex (BA 4), somatosensory association cortex (BA 5), and visuo-motor areas (BA 7).

To further explore the neural sources of differences in the early phase of error monitoring between tasks, we calculated paired contrasts. Contrast analysis revealed that, compared to the flanker task, the go/no-go task was characterized by increased activation in the left and right visuo-motor areas (BA 7) and right somatosensory association cortex (BA 5), the center of mass of the significant cluster located at MNI coordinates (XYZ) = -16.9, 43.5, 67.6; t(207) = -4.89; FDR corrected $p < 0.001$. Significantly increased activation was also observed in the left visual areas (BA 17–19; Fig. 3B).

Compared to the stop-signal task, the go/no-go task showed increased activation in the premotor cortex and SMA (BA 6) in a cluster of 2,951 voxels, with the center of mass at MNI coordinates (XYZ) = 0.9, 96.1, 11.9; t(207) = -4.65; FDR corrected $p < 0.001$. Additional significant clusters included voxels in the left primary sensory areas (BA 1), primary motor cortex (BA 4), somatosensory association cortex (BA 5), and visuo-motor areas (BA 7). Similarly to contrast with the flanker task, increased activation was also found in clusters involving visual areas (BA 17, 18; Fig. 3C).

When comparing neural activity between the flanker and stop-signal tasks, we found increased activation in the flanker task in the ventral ACC (BA 24) in a cluster of 831 voxels, with the center of mass at MNI coordinates (XYZ) = -8.5, -5.3, 38.8; t(207) = 3.80; FDR corrected p = 0.020. We also observed an increased activation in the left premotor cortex and SMA (BA 6) and in the left primary sensory areas (BA 1). In contrast, we have found decreased activity in the dACC (BA 32) in a cluster of 138 voxels, center of mass at MNI coordinates (XYZ) = -4.0, -14.2, 32.8; t(207) = 3.35; FDR corrected p = 0.032 (see Fig. 3D).

Discussion

In this study, we examined whether the early phase of error monitoring reflects a common neural mechanism across inhibitory tasks or a combination of task-specific processes related to distinct types of cognitive failures. We demonstrated that (1) the early phase of error monitoring in tasks requiring response withholding (go/no-go task) and response selection (flanker task) share similar spatiotemporal activity patterns, unlike in tasks requiring response cancellation (stop-signal task), (2) overlapping brain areas activated across all three inhibitory control tasks primarily involve the (pre-)SMA, and (3) error monitoring in different types of inhibitory control triggers also task-specific brain activity.

The neural activity associated with the early phase of error monitoring, irrespective of task type, primarily involved the pre-SMA, SMA, primary sensory areas, primary motor cortex, somatosensory association cortex, and visuo-motor areas. While the latter regions are primarily implicated in motor response initiation and control, the pre-SMA and SMA have been increasingly recognized as key neural sources of error monitoring (Bonini et al., 2014; Coull, Vidal, & Burle, 2016; Fu et al., 2019; Iannaccone et al., 2015; Ullsperger & von Cramon, 2001) and inhibitory control of unwanted actions (Cieslik et al., 2015; Swick et al., 2011). As Coull et al. noted, the role of SMA in action control positions it ideally to access information about the outcomes of inhibition processes. Our results further support this view, highlighting the role of the SMA and pre-SMA in evaluating action outcomes and indicating that this engagement is independent of inhibitory control type.

Although ERN-related brain activity in the go/no-go and flanker tasks was characterized by the same microstate, source analysis revealed differences in the neural sources contributing to this activity. These differences were observed in right visuo-motor areas, right somatosensory association areas, and left visual areas. Further, increased activity in the ventral ACC and dACC was observed during the flanker task compared to the go/no-go task, though this difference did not surpass the whole-brain corrected threshold for significance. These results suggest that the main differences in the early phase of error monitoring between tasks requiring response withholding and selection are confined to motor and visual areas. Thus, they may arise more from differences in the stimuli processing and response execution methods between the two tasks rather than from error monitoring itself, which likely relies on similar cognitive processes.

Action cancellation, unlike response selection and withholding, requires inhibiting an ongoing action in response to stop signal presented after a go stimulus. Previous studies have suggested that the time difference in presenting no-go and stop signals leads to distinct activation patterns between response withholding and cancellation, e.g., increased activation in the right inferior and superior frontal gyri (SFG; Swick et al., 2011; Rubia et al., 2001).

In our study, the ERN-related brain activity in the stop-signal task was assigned to a distinct cluster compared to the go/no-go and flanker tasks. Thus, the microstate analysis results support the idea of distinct activation patterns between response withholding and cancellation. However, while the SFG showed increased activity during the stop-signal task compared to the other tasks (see Fig. 3A, yellow cluster), this difference did not exceed the whole-brain corrected threshold for significance. The main significant difference between the go/no-go and stop-signal tasks was found in the activity of the SMA, which was reduced in the stop-signal task compared to the go/no-go task. The SMA is typically associated with body movement representation (Nachev, Kennard, & Husain, 2008). However, according to the "what-when-whether" model (Zapparoli, Seghezzi, & Paulesu, 2017), SMA might also be specifically involved in processing the timing of inhibition (see also Coull et al., 2016). Consequently, the observed differences in SMA activity could stem from the different timing of the stimuli signaling the need for inhibition in the go/no-go and stop-signal tasks. This suggests that error monitoring in response withholding and cancellation might involve slightly different cognitive processes related to inhibition timing. The activity of the more cognitively involved pre-SMA (Nachev et al., 2008) remains similar across both action withholding and cancellation.

When comparing response cancellation with selection, error monitoring during response selection was linked to stronger activation in the pre-SMA and ventral ACC, whereas action cancellation was associated with greater activity in the dACC. Ventral regions of the ACC are typically linked with proactive control and conflict processing (Alexander & Brown, 2019; Desmet, Fias, & Brass, 2011). Thus, our findings suggest that, error monitoring in tasks requiring response selection under interference maintains prominent conflict-related signals in the ventral ACC. Additionally, increased pre-SMA activity indicates stronger error monitoring during response selection than cancellation.

In contrast, the stronger engagement of the dACC during response cancellation may reflect more reactive control (Shenhav et al., 2014), driven by choice difficulty, prediction error, and the negative surprise evoked by the unexpected stop signal presentation. The timing and interplay between the go response and stop signal presentation in the stop-signal task may lead to the simultaneous activation of both stop-related surprise and error monitoring signals. Indeed, Clayson et al. (2023) demonstrated a close association between the stop-related N2 ERP component and the ERN. Our results suggest that error-related activity in the stop-signal task may reflect a combination of stop-related and response evaluation signals. However, the activity of the dACC is not necessarily linked to the stop-related surprise signal, and the relationship and overlap between stopping and monitoring signals remains an ongoing debate (Maruo, Sommer, & Masaki, 2017; Maruo & Masaki, 2022).

Conclusions

Our findings revealed that the early phase of error monitoring is not uniform across different contexts. Significant differences in the neural sources estimated for ERN-related microstates across the three tasks suggest that error monitoring involves multiple cognitive processes, depending on the type of inhibitory control. Consequently, the early phase of error monitoring should be viewed as a collection of interconnected cognitive processes rather than a single cognitive process. A key limitation of this study is the lack of individualized boundary element models, such as participant-specific MRIs. While this reduce anatomical precision of our results, we believe that the large sample size facilitate meaningful interpretation of the group-level results.

Acknowledgments

We gratefully acknowledge the help of students and collaborators from Jagiellonian University with the data recording. We are also grateful to the participants who volunteered to take part in the study. This study was supported by a Sonata Bis 10 grant (2020/38/E/HS6/00490) from the National Science Centre of Poland awarded to Magdalena Senderecka.

References

Alexander, W. H., & Brown, J. W. (2019). The Role of the Anterior Cingulate Cortex in Prediction Error and Signaling Surprise. *Topics in Cognitive Science*, *11*(1), 119–135. doi: 10.1111/tops.12307

Antonova, I., van Swam, C., Hubl, D., Griskova-Bulanova, I., Dierks, T., & Koenig, T. (2021). Altered Visuospatial Processing in Schizophrenia: An Event-related Potential Microstate Analysis Comparing Patients with and without Hallucinations with Healthy Controls. *Neuroscience*, *479*, 140–156. doi: 10.1016/j.neuroscience.2021.10.014

Bagdasarov, A., Roberts, K., Brunet, D., Michel, C. M., & Gaffrey, M. S. (2024). Exploring the Association Between EEG Microstates During Resting-State and Error-Related Activity in Young Children. *Brain Topography*, *37*(4), 552–570. doi: 10.1007/s10548-023-01030-2

Bagdasarov, A., Roberts, K., Bréchet, L., Brunet, D., Michel, C. M., & Gaffrey, M. S. (2022). Spatiotemporal dynamics of EEG microstates in four- to eight-year-old children: Age- and sex-related effects. *Developmental Cognitive Neuroscience*, *57*, 101134. doi: 10.1016/j.dcn.2022.101134

BMJ. (1996). Declaration of Helsinki (1964). *BMJ*, *313*(7070), 1448–1449. doi: 10.1136/bmj.313.7070.1448a

Bonini, F., Burle, B., Liégeois-Chauvel, C., Régis, J., Chauvel, P., & Vidal, F. (2014). Action monitoring and medial frontal cortex: leading role of supplementary motor area. *Science (New York, N.Y.)*, *343*(6173), 888–891. doi: 10.1126/science.1247412

Brazdil, M., Roman, R., Daniel, P., & Rektor, I. (2005). Intracerebral Error-Related Negativity in a Simple Go/NoGo Task. *Journal of Psychophysiology*, *19*, 244–255. doi: 10.1027/0269-8803.19.4.244

Brunet, D., Murray, M. M., & Michel, C. M. (2011). Spatiotemporal analysis of multichannel EEG: CARTOOL. *Computational Intelligence and Neuroscience*, *2011*, 813870. doi: 10.1155/2011/813870

Bréchet, L., Brunet, D., Perogamvros, L., Tononi, G., & Michel, C. M. (2020). EEG microstates of dreams. *Scientific Reports*, *10*(1), 17069. doi: 10.1038/s41598-020-74075-z

Cieslik, E. C., Mueller, V. I., Eickhoff, C. R., Langner, R., & Eickhoff, S. B. (2015). Three key regions for supervisory attentional control: evidence from neuroimaging meta-analyses. *Neuroscience and Biobehavioral Reviews*, *48*, 22–34. doi: 10.1016/j.neubiorev.2014.11.003

Clayson, P. E., Mcdonald, J. B., Park, B., Holbrook, A., Baldwin, S. A., Riesel, A., & Larson, M. J. (2023). Registered replication report of the construct validity of the error-related negativity (ERN): A multi-site study of task-specific ERN correlations with internalizing and externalizing symptoms. *Psychophysiology*, e14496. doi: 10.1111/psyp.14496

Coull, J. T., Vidal, F., & Burle, B. (2016). When to act, or not to act: that's the SMA's question. *Current Opinion in Behavioral Sciences*, *8*, 14–21. doi: 10.1016/j.cobeha.2016.01.003

Dehaene, S., Posner, M. I., & Tucker, D. M. (1994). Localization of a Neural System for Error Detection and Compensation. *Psychological Science*, *5*(5), 303–305. doi: 10.1111/j.1467-9280.1994.tb00630.x

Desmet, C., Fias, W., & Brass, M. (2011). Performance monitoring at the task and the response level. *Reviews in the Neurosciences*, *22*(5), 575–581. doi: 10.1515/RNS.2011.040

Endrass, T., & Ullsperger, M. (2014). Specificity of performance monitoring changes in obsessive-compulsive disorder. *Neuroscience and Biobehavioral Reviews*, *46 Pt 1*, 124–138. doi: 10.1016/j.neubiorev.2014.03.024

Eriksen, B. A., & Eriksen, C. W. (1974). Effects of noise letters upon the identification of a target letter in a nonsearch task. *Perception & Psychophysics*, *16*(1), 143–149. doi: 10.3758/BF03203267

Fiehler, K., Ullsperger, M., & Von Cramon, D. Y. (2005). Electrophysiological correlates of error correction. *Psychophysiology*, *42*(1), 72–82. doi: 10.1111/j.1469-8986.2005.00265.x

Foti, D., Kotov, R., Bromet, E., & Hajcak, G. (2012). Beyond the broken error-related negativity: Functional and diagnostic correlates of error processing in psychosis. *Biological Psychiatry*, *71*(10), 864–872. doi: 10.1016/j.biopsych.2012.01.007

Fu, Z., Wu, D.-A. J., Ross, I., Chung, J. M., Mamelak, A. N., Adolphs, R., & Rutishauser, U. (2019). Single-Neuron Correlates of Error Monitoring and Post-Error Adjustments in Human Medial Frontal Cortex. *Neuron*, *101*(1), 165–177.e5. doi: 10.1016/j.neuron.2018.11.016

Gehring, W. J., Goss, B., Coles, M. G. H., Meyer, D. E., & Donchin, E. (1993). A Neural System for Error Detection and Compensation. *Psychological Science*, *4*(6), 385–390. doi: 10.1111/j.1467-9280.1993.tb00586.x

Grabowska, A., Sondej, F., Haaf, J., Nunez, M., & Senderecka, M. (2025). Individual differences in neurophysiological correlates of post-response adaptation: A model-based approach. *OSF*. doi: 10.31234/osf.io/7m8r9_v1

Grabowska, A., Sondej, F., & Senderecka, M. (2024). A network analysis of affective and motivational individual differences and error monitoring in a non-clinical sample. *Cerebral Cortex*, *34*(10). doi: 10.1093/cercor/bhae397

Grabowska, A., Zabielski, J., & Senderecka, M. (2024).

Machine learning reveals differential effects of depression and anxiety on reward and punishment processing. *Scientific Reports*, *14*(1), 8422. (Publisher: Nature Publishing Group) doi: 10.1038/s41598-024-58031-9

Gratton, G., Coles, M. G. H., & Donchin, E. (1983). A new method for off-line removal of ocular artifact. *Electroencephalography and Clinical Neurophysiology*, *55*(4), 468–484. doi: 10.1016/0013-4694(83)90135-9

Hajcak, G., Franklin, M. E., Foa, E. B., & Simons, R. F. (2008). Increased error-related brain activity in pediatric obsessive-compulsive disorder before and after treatment. *The American Journal of Psychiatry*, *165*(1), 116–123. doi: 10.1176/appi.ajp.2007.07010143

Iannaccone, R., Hauser, T. U., Staempfli, P., Walitza, S., Brandeis, D., & Brem, S. (2015). Conflict monitoring and error processing: new insights from simultaneous EEG-fMRI. *NeuroImage*, *105*, 395–407. doi: 10.1016/j.neuroimage.2014.10.028

Logan, G. D., & Cowan, W. B. (1984). On the ability to inhibit thought and action: A theory of an act of control. *Psychological Review*, *91*(3), 295–327. doi: 10.1037/0033-295X.91.3.295

Maruo, Y., & Masaki, H. (2022). A possibility of error-related processing contamination in the No-go N2: The effect of partial-error trials on response inhibition processing. *The European Journal of Neuroscience*, *55*(8), 1934–1946. doi: 10.1111/ejn.15658

Maruo, Y., Sommer, W., & Masaki, H. (2017). The effect of monetary punishment on error evaluation in a Go/No-go task. *International Journal of Psychophysiology*, *120*, 54–59. doi: 10.1016/j.ijpsycho.2017.07.002

Michel, C. M., & Brunet, D. (2019). EEG Source Imaging: A Practical Review of the Analysis Steps. *Frontiers in Neurology*, *10*, 325. doi: 10.3389/fneur.2019.00325

Michel, C. M., & Koenig, T. (2018). EEG microstates as a tool for studying the temporal dynamics of whole-brain neuronal networks: A review. *NeuroImage*, *180*, 577–593. doi: 10.1016/j.neuroimage.2017.11.062

Nachev, P., Kennard, C., & Husain, M. (2008). Functional role of the supplementary and pre-supplementary motor areas. *Nature Reviews. Neuroscience*, *9*(11), 856–869. doi: 10.1038/nrn2478

Nash, K., Kleinert, T., Leota, J., Scott, A., & Schimel, J. (2022). Resting-state networks of believers and non-believers: An EEG microstate study. *Biological Psychology*, *169*, 108283. doi: 10.1016/j.biopsycho.2022.108283

Nash, K., Leota, J., Kleinert, T., & Hayward, D. A. (2023). Anxiety disrupts performance monitoring: integrating behavioral, event-related potential, EEG microstate, and sLORETA evidence. *Cerebral Cortex*, *33*(7), 3787–3802. doi: 10.1093/cercor/bhac307

Olvet, D. M., & Hajcak, G. (2008). The error-related negativity (ERN) and psychopathology: Toward an endophenotype. *Clinical Psychology Review*, *28*(8), 1343–1354. doi: 10.1016/j.cpr.2008.07.003

Pascual-Marqui, R. D. (2002). Standardized low-resolution brain electromagnetic tomography (sLORETA): technical details. *Methods and Findings in Experimental and Clinical Pharmacology*, *24 Suppl D*, 5–12.

Pourtois, G. (2011). Early Error Detection Predicted by Reduced Pre-response Control Process: An ERP Topographic Mapping Study. *Brain Topography*, *23*(4), 403–422. doi: https://doi.org/10.1007/s10548-010-0159-5

Ridderinkhof, K. R., Nieuwenhuis, S., & Bashore, T. R. (2003). Errors are foreshadowed in brain potentials associated with action monitoring in cingulate cortex in humans. *Neuroscience Letters*, *348*(1), 1–4. doi: 10.1016/S0304-3940(03)00566-4

Riesel, A. (2019). The erring brain: Error-related negativity as an endophenotype for OCD-A review and meta-analysis. *Psychophysiology*, *56*(4), e13348. doi: 10.1111/psyp.13348

Riesel, A., Weinberg, A., Endrass, T., Meyer, A., & Hajcak, G. (2013). The ERN is the ERN is the ERN? Convergent validity of error-related brain activity across different tasks. *Biological Psychology*, *93*(3), 377–385. doi: 10.1016/j.biopsycho.2013.04.007

Rosvold, H. E., Mirsky, A. F., Sarason, I., Bransome Jr., E. D., & Beck, L. H. (1956). A continuous performance test of brain damage. *Journal of Consulting Psychology*, *20*(5), 343–350. doi: 10.1037/h0043220

Rubia, K., Russell, T., Overmeyer, S., Brammer, M. J., Bullmore, E. T., Sharma, T., … Taylor, E. (2001). Mapping Motor Inhibition: Conjunctive Brain Activations across Different Versions of Go/No-Go and Stop Tasks. *NeuroImage*, *13*(2), 250–261. doi: 10.1006/nimg.2000.0685

Segalowitz, S. J., Santesso, D. L., Murphy, T. I., Homan, D., Chantziantoniou, D. K., & Khan, S. (2010). Retest reliability of medial frontal negativities during performance monitoring. *Psychophysiology*, *47*(2), 260–270. doi: 10.1111/j.1469-8986.2009.00942.x

Senderecka, M., Grabowska, A., Szewczyk, J., Gerc, K., & Chmylak, R. (2012). Response inhibition of children with ADHD in the stop-signal task: an event-related potential study. *International Journal of Psychophysiology: Official Journal of the International Organization of Psychophysiology*, *85*(1), 93–105. doi: 10.1016/j.ijpsycho.2011.05.007

Shenhav, A., Straccia, M. A., Cohen, J. D., & Botvinick, M. M. (2014). Anterior cingulate engagement in a foraging context reflects choice difficulty, not foraging value. *Nature Neuroscience*, *17*(9), 1249–1254. doi: 10.1038/nn.3771

Stroop, J. R. (1935). Studies of interference in serial verbal reactions. *Journal of Experimental Psychology*, *18*(6), 643–662. doi: 10.1037/h0054651

Swick, D., Ashley, V., & Turken, U. (2011). Are the neural correlates of stopping and not going identical? Quantitative meta-analysis of two response inhibition tasks. *NeuroImage*, *56*(3), 1655–1665. doi: 10.1016/j.neuroimage.2011.02.070

Ullsperger, M., Danielmeier, C., & Jocham, G. (2014). Neurophysiology of performance monitoring and adaptive behavior. *Physiological Reviews*, *94*(1), 35–79. doi: 10.1152/physrev.00041.2012

Ullsperger, M., & von Cramon, D. Y. (2001). Subprocesses of Performance Monitoring: A Dissociation of Error Processing and Response Competition Revealed by Event-Related fMRI and ERPs. *NeuroImage*, *14*(6), 1387–1401. doi: 10.1006/nimg.2001.0935

van Meel, C. S., Heslenfeld, D. J., Oosterlaan, J., & Sergeant, J. A. (2007). Adaptive control deficits in attention-deficit/hyperactivity disorder (ADHD): The role of error processing. *Psychiatry Research*, *151*(3), 211–220. doi: 10.1016/j.psychres.2006.05.011

Verbruggen, F., Aron, A. R., Band, G. P., Beste, C., Bissett, P. G., Brockett, A. T., ... Boehler, C. N. (2019). A consensus guide to capturing the ability to inhibit actions and impulsive behaviors in the stop-signal task. *eLife*, *8*, e46323. doi: 10.7554/eLife.46323

Vocat, R., Pourtois, G., & Vuilleumier, P. (2008). Unavoidable errors: A spatio-temporal analysis of time-course and neural sources of evoked potentials associated with error processing in a speeded task. *Neuropsychologia*, *46*(10), 2545–2555. doi: https://doi.org/10.1016/j.neuropsychologia.2008.04.006

Zapparoli, L., Seghezzi, S., & Paulesu, E. (2017). The What, the When, and the Whether of Intentional Action in the Brain: A Meta-Analytical Review. *Frontiers in Human Neuroscience*, *11*, 238. doi: 10.3389/fnhum.2017.00238

Zhang, R., Geng, X., & Lee, T. M. C. (2017). Large-scale functional neural network correlates of response inhibition: an fMRI meta-analysis. *Brain Structure and Function*, *222*(9), 3973–3990. doi: 10.1007/s00429-017-1443-x